A&A 561, L3 (2014)
DOI: 10.1051/0004-6361/201322883

Astronomy & Astrophysics

Letter to the Editor

Multiplicity of Galactic Cepheids from long-baseline interferometry

II. The Companion of AX Circini revealed with VLTI/PIONIER⋆,⋆⋆

A. Gallenne[1], A. Mérand[2], P. Kervella[3], J. Breitfelder[2,3], J.-B. Le Bouquin[4], J. D. Monnier[5], W. Gieren[1], B. Pilecki[1,6], and G. Pietrzyński[1,6]

[1] Universidad de Concepción, Departamento de Astronomía, Casilla 160-C, Concepción, Chile
e-mail: agallenne@astro-udec.cl
[2] European Southern Observatory, Alonso de Córdova 3107, Casilla 19001, Santiago 19, Chile
[3] LESIA, Observatoire de Paris, CNRS UMR 8109, UPMC, Université Paris Diderot, 5 place Jules Janssen, 92195 Meudon, France
[4] UJF-Grenoble 1/CNRS-INSU, Institut de Planétologie et d'Astrophysique de Grenoble (IPAG) UMR 5274, Grenoble, France
[5] Astronomy Department, University of Michigan, 1034 Dennison Bldg, Ann Arbor, MI 48109-1090, USA
[6] Warsaw University Observatory, Al. Ujazdowskie 4, 00-478 Warsaw, Poland

Received 21 October 2013 / Accepted 6 December 2013

ABSTRACT

Aims. We aim at detecting and characterizing the main-sequence companion of the Cepheid AX Cir ($P_{\rm orb} \sim 18$ yrs). The long-term objective is to estimate the mass of both components and the distance to the system.
Methods. We used the PIONIER combiner at the VLT Interferometer to obtain the first interferometric measurements of the short-period Cepheid AX Cir and its orbiting component.
Results. The companion is resolved by PIONIER at a projected separation $\rho = 29.2 \pm 0.2$ mas and projection angle PA $= 167.6 \pm 0.3°$. We measured H-band flux ratios between the companion and the Cepheid of $0.90 \pm 0.10\%$ and $0.75 \pm 0.17\%$, at pulsation phases for the Cepheid of $\phi = 0.24$ and 0.48, respectively. The lower contrast at $\phi = 0.48$ is due to the increased brightness of the Cepheid compared to $\phi = 0.24$. This gives an average apparent magnitude $m_{\rm H}$(comp) $= 9.06 \pm 0.24$ mag. The limb-darkened angular diameter of the Cepheid at the two pulsation phases was measured to be $\theta_{\rm LD} = 0.839 \pm 0.023$ mas and $\theta_{\rm LD} = 0.742 \pm 0.020$ mas, at $\phi = 0.24$ and 0.48, respectively. A lower limit on the total mass of the system was also derived based on our measured separation, and we found $M_{\rm T} \geq 9.7 \pm 0.6\ M_{\odot}$.

Key words. techniques: interferometric – techniques: high angular resolution – stars: variables: Cepheids – binaries: close

1. Introduction

Cepheids are powerful astrophysical laboratories that provide fundamental clues for studying the pulsation and evolution of intermediate-mass stars. However, the discrepancy between masses predicted by stellar evolutionary and pulsation models is still not understood well. The most cited scenarios to explain this discrepancy are a mass-loss process during the Cepheid's evolution and/or convective a core overshooting during the main-sequence stage (Neilson et al. 2011; Keller 2008; Bono et al. 2006). Therefore, accurate masses of a few percent are needed to help constrain the two models.

So far, the mass of only one Cepheid, Polaris, has been measured (Evans et al. 2008); otherwise, they are derived through the mass of the companion inferred from a mass-temperature relation. When in binary systems, Cepheids offer the unique opportunity to make progress in resolving the Cepheid mass problem. The dynamical masses can be estimated (Pietrzyński et al. 2011, 2010; Evans et al. 2008), and provide new constraints on evolution and pulsation theory (e.g. Prada Moroni et al. 2012). This gives new insight on the Cepheid mass, and can settle the discrepancy between pulsation and evolution models. Binary systems are also valuable tools to obtain independent distance measurements of Cepheids, needed to calibrate the Leavitt Law.

However, most of the companions are hot main-sequence stars, and are located too close to the Cepheid (∼1−40 mas) to be observed with a 10-m class telescope at optical wavelengths. The already existing orbit measurements were estimated only from IUE spectrum or from the radial velocity variations. The only way to spatially resolve such systems is to use long-baseline interferometry or aperture masking. We started a long-term interferometric observing program that aims at studying a sample of northern and southern binary Cepheids. The first goal is to determine the angular separation and the apparent brightness ratio from the interferometric visibility and closure phase measurements. Our long-term objective is to determine the full set of orbital elements, absolute masses and geometric distances. Our program started in 2012 and has already provided new informations on the V1334 Cyg Cepheid system (Gallenne et al. 2013, hereafter Paper I).

In this second paper, we report the detection of the orbiting companion around the Cepheid AX Cir (HD 130701, HR 5527). This pulsating star has a spectroscopic companion, first suspected from composite spectra by Jaschek & Jaschek (1960), and later confirmed by Lloyd Evans (1982). A preliminary orbital period of about 4600 days was then estimated by Szabados (1989). Bohm-Vitense & Proffitt (1985) and Evans (1994) also

⋆ Based on observations made with ESO telescopes at Paranal observatory under program ID 090.D-0010.
⋆⋆ Table 2 is available in electronic form at http://www.aanda.org

Table 1. Parameters of the Cepheid and its close companion.

Primary (Cepheid)							Secondary[f]						
$\overline{m}_V$[a]	$\overline{m}_K$[b]	$\overline{m}_H$[b]	Sp. Type[c]	P_{pul}[c] (days)	$\overline{\theta}_{LD}$[d] (mas)	d[e] (pc)	Sp. Type	P_{orb} (days)	T_0 (days)	e	$a_1 \sin i$ (AU)	ω (rad)	$f(M)$ ($M_\odot$)
5.89	3.76	3.85	F8II	5.2733	0.76	500	B6V	6532	2 448 500	0.19	6.05	4.03	0.68

Notes. $\overline{m}_V$, $\overline{m}_K$, $\overline{m}_H$: mean apparent V, K and H magnitudes. Sp. Type: spectral type. P_{pul}: period of pulsation. $\overline{\theta}_{LD}$: mean angular diameter. d: distance. P_{orb}: orbital period. T_0: time passage through periastron. e: eccentricity of the orbit. $a_1 \sin i$: projected semi-major axis of the orbit of the Cepheid about the center of mass of the system. ω: argument of periastron. $f(M)$: spectroscopic mass function.

References. [(a)] From Klagyivik & Szabados (2009). [(b)] From the 2MASS catalog (Cutri et al. 2003). [(c)] From Samus et al. (2009). [(d)] From Gallenne et al. (2011, at $\phi = 0.27$). [(e)] From the K-band P-L relation of Storm et al. (2011). [(f)] From Evans (2000) and Petterson et al. (2004).

detected the companion from International Ultraviolet Exporer (IUE) low-resolution spectra, and set its spectral type to be a B6V star. The first orbital solution was provided by Petterson et al. (2004) from precise and homogeneous high-resolution spectroscopic measurements; however, it does not include the semi-major axis, the inclination angle, and the longitude of the ascending node, which can only be provided from astrometry. We list some parameters of the AX Cir system in Table 1.

We present here the first spatially resolved detection of this companion from VLTI/PIONIER observations. We first describe in Sect. 2 the beam combiner, the observations, and the raw data calibration. In Sect. 3 we explain the data analysis and present our results. We then discuss our measured flux ratio and projected separation, and conclude in Sect. 5.

2. Observations and data reduction

We used the Very Large Telescope Interferometer (VLTI; Haguenauer et al. 2010) with the four-telescope combiner PIONIER (Le Bouquin et al. 2011) to measure squared visibilities and closure phases of the AX Cir binary system. PIONIER combines the light coming from four telescopes in the H band, either in a broad band mode or with a low spectral resolution, where the light is dispersed into three or seven spectral channels. The recombination provides simultaneously six visibilities and four closure phase signals per spectral channel.

Our observations were carried out on UT 2013 July 11 and 14, with dispersed fringes in three spectral channels. All observations made use of the 1.8 m Auxiliary Telescopes with the configuration K0-A1-G1-J3 and D0-G1-H0-I1, providing six projected baselines ranging from 40 to 140 m. To monitor the instrumental and atmospheric contributions, the standard procedure, which consists of interleaving the science target by reference stars, was used. The calibrators, HD 133869 and HD 129462, were selected using the *SearchCal*[1] software (Bonneau et al. 2006, 2011) provided by the JMMC. The journal of the observations is presented in Table 2 and the (u, v) plane covered by the observations is shown in Fig. 1. We have collected a total of 435 squared visibility and 300 closure phase measurements.

The data have been reduced with the *pndrs* package described in Le Bouquin et al. (2011). The main procedure is to compute squared visibilities and triple products for each baseline and spectral channel, and to correct for photon and readout noises. The final calibrated closure phases of July 14 are presented in Fig. 3. The variations in the signal suggest the presence of the companion, and this is strengthened by a higher signal-to-noise ratio when combining all the data.

[1] Available at http://www.jmmc.fr/searchcal

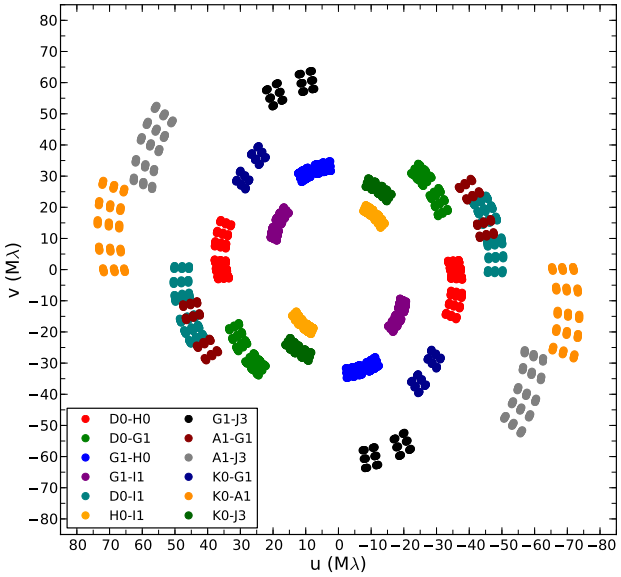

Fig. 1. (u, v) plane coverage for all our observations of AX Cir.

3. Model fitting

The squared visibilities and closure phase signals were modeled assuming a uniform disk (UD) angular diameter for the Cepheid (the primary) plus a point source companion. The fitted parameters are the angular diameter of the Cepheid θ_{UD}, the relative position of the component $(\Delta\alpha, \Delta\delta)$, and the flux ratio $f = f_{com}/f_{cep}$. The coherence loss effect due to spectral smearing on the companion was also modeled using the function $|\mathrm{sinc}x|$, where $x = \pi(u\Delta\alpha + v\Delta\delta)/(\lambda R)$ at spectral resolution $R = 18$ and spatial frequencies (u, v).

The choice of a UD diameter for the Cepheid instead of a limb-darkened (LD) disk for the fitting procedure is justified because the angular diameter is small compared to the angular resolution of the interferometer, and the limb darkening effects are therefore undetectable. The conversion from UD to LD angular diameter was done afterwards by using a linear-law parametrization $I_\lambda(\mu) = 1 - u_\lambda(1 - \mu)$, with the LD coefficient $u_\lambda = 0.2887$ (Claret & Bloemen 2011) for both epochs, and using the stellar parameters $T_{eff} = 5400$ K, $\log g = 2.0$, [Fe/H] = 0.0, and $v_t = 5$ km s^{-1} (Usenko et al. 2011; Acharova et al. 2012). The conversion is then given by the approximate formula of Hanbury Brown et al. (1974):

$$\theta_{LD}(\lambda) = \theta_{UD}(\lambda)\sqrt{\frac{1 - u_\lambda/3}{1 - 7u_\lambda/15}}.$$

Changing T_{eff} by ±400 k changes the diameter by less than 0.2%, well below our measured uncertainties.

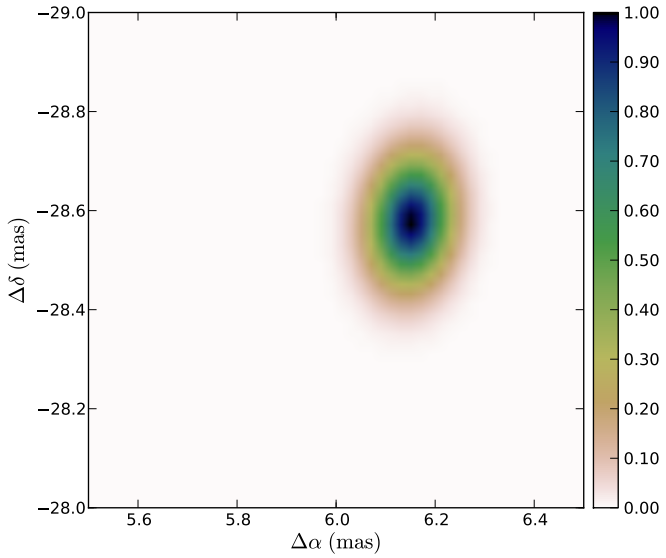

Fig. 2. Probability map for the companion position of July 14.

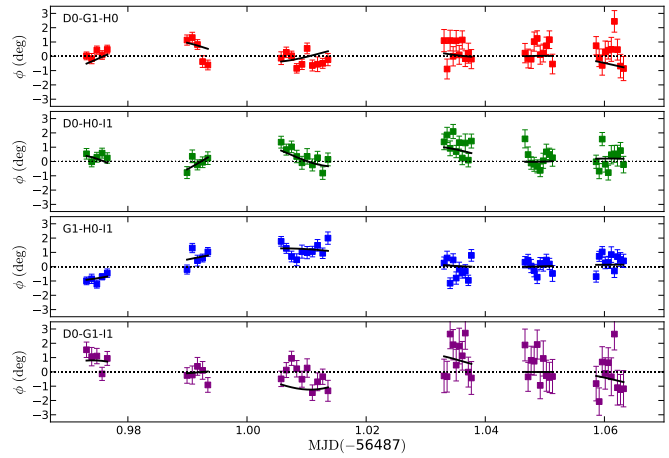

Fig. 3. Closure phase signal of AX Cir for July 14, with respect to the modified Julian date. The spectral channels were averaged for clarity. The solid black line represents our best fit model.

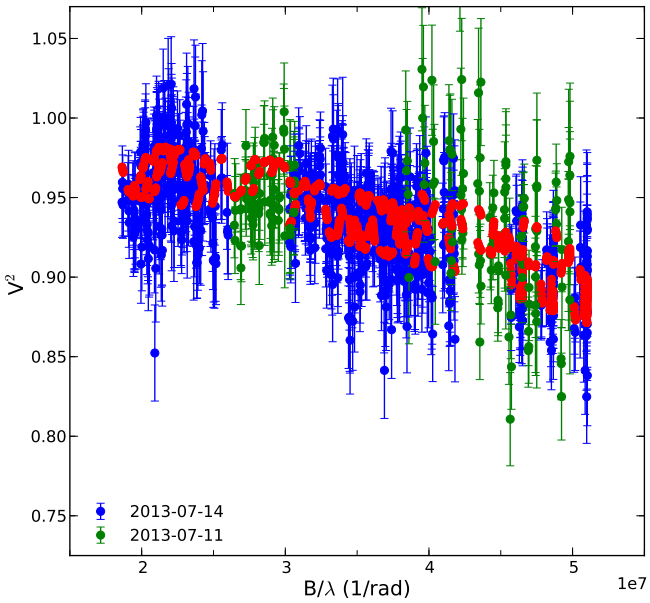

Fig. 4. Squared visibility measurements of AX Cir. The data are in blue for July 14 and in green for July 11, while the red dots are the fitted binary model for both epochs.

Table 3. Final best-fit parameters.

	2013-07-11	2012-07-14
Single star model		
$\theta_{\rm UD}$ (mas)	0.770 ± 0.016	0.931 ± 0.019
$\theta_{\rm LD}$ (mas)	0.787 ± 0.016	0.952 ± 0.020
χ^2_r	1.45	1.09
Binary model		
$\theta_{\rm UD}$ (mas)	0.726 ± 0.020	0.821 ± 0.022
$\theta_{\rm LD}$ (mas)	0.742 ± 0.020	0.839 ± 0.023
f (%)	0.75 ± 0.17	0.90 ± 0.10
$\Delta\alpha$ (mas)	6.421 ± 0.198	6.153 ± 0.155
$\Delta\delta$ (mas)	−28.366 ± 0.366	−28.584 ± 0.229
χ^2_r	1.17	0.72

Notes. $\theta_{\rm UD}$, $\theta_{\rm LD}$: uniform and limb-darkened disk angular diameter, respectively. f, Δx, Δy: flux ratio and position of the companion. χ^2_r: reduced χ^2 of the corresponding best-fit model.

For each epoch, the fitting procedure was done in two steps. We first proceeded to a 80 × 80 mas grid search in the χ^2 space, with spacing of 0.2 mas, which aims at determining the approximate position of the companion and avoid local minima. Then a finer search of 5 × 5 mas with a 0.05 mas spacing around the most likely position was carried out to obtain the final parameters. We chose $\theta_{\rm UD}$ = 0.76 mas (Gallenne et al. 2011) and f = 1.5% (Evans 1994) as first guesses.

Our model did not take a possible circumstellar envelope (CSE) emission into account, which could lead to an overestimate of the angular diameter. From the spectral energy distribution AX Cir given by Gallenne et al. (2011), the infrared excess caused by the CSE appears around 10 μm, while it is negligible at 1.6 μm (i.e., <2%, which would lead to visibility loss of the same amount at first order, and below our visibility accuracy).

The probability map for the observations of July 14 is shown in Fig. 2, and the fitted parameters for both epochs are reported in Table 3. The companion is clearly detected at the two epochs at coordinates ρ = 29.2 ± 0.2 mas and PA = 167.6 ± 0.3°. The model for the observations of July 14 is represented graphically in Fig. 3. We estimated limb-darkened angular diameters $\theta_{\rm LD}$ = 0.742 ± 0.020 mas and 0.839 ± 0.023 mas, for July 11 and 14, respectively (at pulsation phases ϕ = 0..48 and 0.24, respectively), in agreement with the angular diameter, 0.76 ± 0.03 estimated by Gallenne et al. (2011) at phase ϕ = 0.27. It is also consistent with the average value of 0.84 mas estimated from the surface brightness relation of Kervella et al. (2004, using magnitudes from Table 1). However, no IR photometric measurements were available at the time of our interferometric observations, and we cannot compare our measured diameters to those derived from surface brightness relationships. Uncertainties were estimated using the subsample bootstrap technique with replacement and 10 000 subsamples. The medians of the probability distribution of the parameters match the best-fit values very well, and we used the maximum value between the 16% and 84% percentiles as uncertainty estimates (although the distributions were roughly symmetrical about the median values).

4. Discussion

The measured flux ratios are slightly different between the two epochs, although within the uncertainties. This is because the

Cepheid is slightly brighter at phase $\phi = 0.48$ (July 11) than in $\phi = 0.24$, which makes the contrast a bit lower. Since we do not have H-band light curves to extract the Cepheid magnitude at a given phase, we took an average to estimate a mean contrast $f = 0.83 \pm 0.14\%$. This gives a difference in apparent magnitude of $\Delta m_{\rm H} = 5.20 \pm 0.18$ mag. This converts to apparent magnitudes for each component by using the 2MASS magnitude as a measure of the combined flux and the following equations:

$$m_1 = m_{12} + 2.5\log(1+f) \quad (1)$$

$$m_2 = m_{12} + 2.5\log(1+1/f) \quad (2)$$

where m_{12} is the 2MASS measurements, and m_1 and m_2 the apparent magnitude of the Cepheid and the component, respectively. We obtain $H_{\rm comp} = 9.06 \pm 0.24$ mag and $H_{\rm cep} = 3.86 \pm 0.24$ mag. The quoted errors are due to the uncertainties in 2MASS. We determined the dereddened magnitude, $H_0^{\rm comp} = 8.94 \pm 0.24$ mag and $H_0^{\rm cep} = 3.72 \pm 0.24$ mag, by adopting the reddening law from Fouqué et al. (2007) with a total-to-selective absorption in the V band of $R_{\rm V} = 3.23$ (Sandage et al. 2004) and a color excess $E(B-V) = 0.262$ from Tammann et al. (2003). From the distance $d = 500 \pm 10$ pc given by the K-band period-luminosity relation (Storm et al. 2011, the quoted error is statistical), we obtain an absolute magnitude for the companion $M_{\rm H} = 0.45 \pm 0.24$ mag. Combining the known spectral type B6V with a color-spectral type relation (Ducati et al. 2001), we obtain $M_V = -0.12 \pm 0.24$ mag.

From Kepler's law and assuming our measured projected separation ρ as a lower limit for the angular semi-major axis, that is $a \geq \rho$, a minimal total mass for the system can be derived:

$$M_{\rm T} = M_1 + M_2 \geq \frac{\rho^3 d^3}{P^2},$$

with ρ in arcsecond, d in parsec, and P in year. We therefore derived $M_{\rm T} \geq 9.7 \pm 0.6\, M_\odot$. This is compatible with the $5.1\, M_\odot$ for the Cepheid, predicted from the pulsation mass (Caputo et al. 2005), and with the $5\, M_\odot$ for the companion, inferred from its spectral type.

5. Conclusion

We used the high angular resolution provided by the four-telescope combiner PIONIER to detect the orbiting companion of the short-period cepheid AX Cir. We employed a binary model with a primary represented by a uniform disk and the secondary as an unresolved source. We derived a limb-darkened angular diameter for the Cepheid at two pulsation phases, $\theta_{\rm LD} = 0.839 \pm 0.023$ mas (at $\phi = 0.24$) and $\theta_{\rm LD} = 0.742 \pm 0.020$ mas (at $\phi = 0.48$). We also measured an averaged H-band flux ratio between the companion and the Cepheid, $f = 0.83 \pm 0.14\%$, and the astrometric position of the secondary relative to the primary, $\rho = 29.2 \pm 0.2$ mas and PA $= 167.8 \pm 0.3°$. We also set a lower limit on the total mass of the system based on our measured projected separation. Finally, we pointed out the need of accurate infrared light curves to enable a more precise flux estimate of the companion from the contrast measured from interferometry.

This second detection (after that of V1334 Cyg, Paper I) demonstrates the capabilities of long-baseline interferometers for studying the close-orbit companions of Cepheids. Further interferometric observations will be obtained in the future to cover the orbit, and then combined with radial velocity measurements to derive all orbital elements. For now, only single-line spectroscopic measurements are available, we are also involved in a long-term spectroscopic program to detect the radial velocity of the companion. This will provide an orbital parallax and model-free masses.

Acknowledgements. The authors thank all the people involved in the VLTI project. A.G. acknowledges support from FONDECYT grant 3130361. J.D.M. acknowledges funding from the NSF grants AST-1108963 and AST-0807577. W.G. and G.P. gratefully acknowledge financial support for this work from the BASAL Centro de Astrofísica y Tecnologías Afines (CATA) PFB-06/2007. Support from the Polish National Science Center grant MAESTRO and the Polish Ministry of Science grant Ideas Plus (awarded to G.P.) is also acknowledged. We acknowledge financial support from the Programme National de Physique Stellaire (PNPS) of CNRS/INSU, France. PIONIER was originally funded by the Poles TUNES and SMING of Université Joseph Fourier (Grenoble) and subsequently supported by INSU-PNP and INSU-PNPS. The integrated optics beam combiner is the result of collaboration between IPAG and CEA-LETI based on CNES R&T funding. This research received the support of PHASE, the high angular resolution partnership between ONERA, the Observatoire de Paris, CNRS, and University Denis Diderot Paris 7. This work made use of the SIMBAD and VIZIER astrophysical database from the CDS, Strasbourg, France, and the bibliographic informations from the NASA Astrophysics Data System. This research has made use of the Jean-Marie Mariotti Center `SearchCal` service, co-developed by FIZEAU and LAOG/IPAG. The research leading to these results received funding from the European Research Council under the European Community's Seventh Framework Program (FP7/2007–2013)/ERC grant agreement N° 227224 (PROSPERITY).

References

Acharova, I. A., Mishurov, Y. N., & Kovtyukh, V. V. 2012, MNRAS, 420, 1590
Bohm-Vitense, E., & Proffitt, C. 1985, ApJ, 296, 175
Bonneau, D., Clausse, J.-M., Delfosse, X., et al. 2006, A&A, 456, 789
Bonneau, D., Delfosse, X., Mourard, D., et al. 2011, A&A, 535, A53
Bono, G., Caputo, F., & Castellani, V. 2006, Mem. Soc. Astron. It., 77, 207
Caputo, F., Bono, G., Fiorentino, G., Marconi, M., & Musella, I. 2005, ApJ, 629, 1021
Claret, A., & Bloemen, S. 2011, A&A, 529, A75
Cutri, R. M., Skrutskie, M. F., van Dyk, S., et al. 2003, VizieR Online Data Catalog: II/246
Ducati, J. R., Bevilacqua, C. M., Rembold, S. B., & Ribeiro, D. 2001, ApJ, 558, 309
Evans, N. R. 1994, ApJ, 436, 273
Evans, N. R. 2000, AJ, 119, 3050
Evans, N. R., Schaefer, G. H., Bond, H. E., et al. 2008, AJ, 136, 1137
Fouqué, P., Arriagada, P., Storm, J., et al. 2007, A&A, 476, 73
Gallenne, A., Kervella, P., & Mérand, A. 2011, A&A, 538, A24
Gallenne, A., Monnier, J. D., Mérand, A., et al. 2013, A&A, 552, A21
Haguenauer, P., Alonso, J., Bourget, P., et al. 2010, in SPIE Conf. Ser., 7734
Hanbury Brown, R., Davis, J., Lake, R. J. W., & Thompson, R. J. 1974, MNRAS, 167, 475
Jaschek, M., & Jaschek, C. 1960, PASP, 72, 500
Keller, S. C. 2008, ApJ, 483
Kervella, P., Bersier, D., Mourard, D., et al. 2004, A&A, 428, 587
Klagyivik, P., & Szabados, L. 2009, A&A, 504, 959
Le Bouquin, J.-B., Berger, J.-P., Lazareff, B., et al. 2011, A&A, 535, A67
Lloyd Evans, T. 1982, MNRAS, 199, 925
Neilson, H. R., Cantiello, M., & Langer, N. 2011, A&A, 529, L9
Petterson, O. K. L., Cottrell, P. L., & Albrow, M. D. 2004, MNRAS, 350, 95
Pietrzyński, G., Thompson, I. B., Gieren, W., et al. 2010, Nature, 468, 542
Pietrzyński, G., Thompson, I. B., Graczyk, D., et al. 2011, ApJ, 742, L20
Prada Moroni, P. G., Gennaro, M., Bono, G., et al. 2012, ApJ, 749, 108
Samus, N. N., Durlevich, O. V., et al. 2009, VizieR Online Data Catalog: B/gcvs
Sandage, A., Tammann, G. A., & Reindl, B. 2004, A&A, 424, 43
Storm, J., Gieren, W., Fouqué, P., et al. 2011, A&A, 534, A94
Szabados, L. 1989, Commun. Konkoly Obs. Hungary, 94, 1
Tammann, G. A., Sandage, A., & Reindl, B. 2003, A&A, 404, 423
Usenko, I. A., Kniazev, A. Y., Berdnikov, L. N., & Kravtsov, V. V. 2011, Astron. Lett., 37, 499

Table 2. Journal of the observations.

UT		Star	Configuration
2013 July 11	0:14	AX Cir	K0-A1-G1-J3
	0:27	HD 129462	K0-A1-G1-J3
	0:36	AX Cir	K0-A1-G1-J3
	0:46	HD 129462	K0-A1-G1-J3
	0:58	AX Cir	K0-A1-G1-J3
	1:18	HD 133869	K0-A1-G1-J3
	1:27	AX Cir	K0-A1-G1-J3
	1:39	HD 133869	K0-A1-G1-J3
	1:51	AX Cir	K0-A1-G1-J3
	2:01	HD 133869	K0-A1-G1-J3
2013 July 14	23:07	HD 133869	D0-G1-H0-I1
	23:21	AX Cir	D0-G1-H0-I1
	23:32	HD 129462	D0-G1-H0-I1
	23:45	AX Cir	D0-G1-H0-I1
	23:55	HD 133869	D0-G1-H0-I1
2013 July 15	00:08	AX Cir	D0-G1-H0-I1
	00:24	HD 129462	D0-G1-H0-I1
	00:47	AX Cir	D0-G1-H0-I1
	00:58	HD 133869	D0-G1-H0-I1
	01:07	AX Cir	D0-G1-H0-I1
	01:17	HD 129462	D0-G1-H0-I1
	01:24	AX Cir	D0-G1-H0-I1
	01:35	HD 129462	D0-G1-H0-I1